

Solid state and solution studies of a vanadium(III)-L-cysteine compound and demonstration of its antimetastatic, antioxidant and inhibition of neutral endopeptidase activities

Angelos Papaioannou^a, Manolis Manos^a, Spiros Karkabounas^b, Roman Liasko^b,
Angelos M. Evangelou^b, Isabel Correia^c, Vicky Kalfakakou^{b,*}, João Costa Pessoa^{c,*},
Themistoklis Kabanos^{a,*}

^a Department of Chemistry, Section of Inorganic and Analytical Chemistry, University of Ioannina, 45110 Ioannina, Greece

^b Laboratory of Experimental Physiology, Faculty of Medicine, University of Ioannina, 46110 Ioannina, Greece

^c Centro Química Estrutural, Instituto Superior Técnico, Av. Rovisco Pais, 1049-001 Lisboa, Portugal

Received 12 September 2003; received in revised form 17 February 2004; accepted 18 February 2004

Available online 19 March 2004

Abstract

Reaction of one equivalent of vanadium(III) chloride with three equivalents of L-cysteine(H₂Cys) in methyl alcohol affords a V^{III}-Cys compound that is formulated as [V^{III}(Hcys)₃]·2HCl·2.5H₂O **1**. The solid state characterization of **1** was performed by microanalysis, circular dichroism (CD) and infrared studies as well as room temperature magnetic susceptibility. These studies have shown coordination of each HCys⁻ ligand to the V^{III} atom through an amine nitrogen and a carboxylate oxygen atoms. Solution studies of **1** were carried out in water and methanol by UV–visible, CD and electron paramagnetic resonance (EPR) spectroscopies. According to these studies, it was evident that despite the progressive oxidation of **1** to oxovanadium(IV) species, some V(III) species were also present in solution after several hours. Compound **1**, V^{IV}OSO₄·5H₂O and L-cysteine were examined for their total antioxidant capacity (TAC) and lag time. Compound **1** exhibited significantly greater total antioxidant capacity and lag time values than L-cysteine. V^{IV}OSO₄·5H₂O did not show any total antioxidant capacity or lag time. The inhibition of neutral endopeptidase (NEP) activity caused by **1**, V^{IV}OSO₄·5H₂O and thiorphan was also measured. Compound **1**, at a concentration of 10⁻³ M, showed inhibition of NEP activity as potent as thiorphan at 10⁻⁶ M, while V^{IV}OSO₄·5H₂O in the same concentration exhibited less than 50% inhibitory activity than that of thiorphan at 10⁻⁶ M. Moreover, the antimetastatic effects of compound **1**, L-cysteine and V^{IV}OSO₄·5H₂O were examined on Wistar rats, treated with 3,4-benzopyrene. The results revealed that **1** prevents significantly lung metastases (only 9.5% of animals treated with **1** showed metastases), whereas 47–52% of the rats of the control group and those treated with L-cysteine and V^{IV}OSO₄·5H₂O exhibited metastases.

© 2004 Elsevier Inc. All rights reserved.

Keywords: Vanadium; Cysteine; Antitumor activity; Circular dichroism; Electron paramagnetic resonance

1. Introduction

Vanadium is accumulated in high concentrations in certain sea squirts [1] and mushrooms of the genus *Amanita* [2]. The function of vanadium in these living systems remains as yet unclear, despite the few hypotheses, which have been put forward [3]. Moreover, three classes of vanadium dependent enzymes, namely, nitrogenases

* Corresponding authors. Tel.: +30-2651-98415; fax: +30-2651-44831 (T. Kabanos), Tel.: +361-21-8464455; fax: +361-21-84644457 (J. Costa Pessoa), Tel.: +30-2651-97579; fax: +30-2651-97850 (V. Kalfakakou).

E-mail addresses: vkalfaka@cc.uoi.gr (V. Kalfakakou), pcjpessoa@mail.ist.utl.pt (J. Costa Pessoa), tkampano@cc.uoi.gr (T. Kabanos).

[4], haloperoxidases [5], and nitrate reductases [6] have been discovered in nature. In addition, vanadium has the ability to produce significant physiological effects, such as the inhibition of phosphate-metabolizing enzymes [7], the stimulation of phosphomutases and – isomerases [8], insulinomimetic activity [9], etc. Vanadium compounds also exhibit significant anticancer activity [10,11]. More specifically, vanadium possesses preventive and therapeutic effects against malignancy, in experimentally induced tumors and malignant cell lines [10]. Various vanadium complexes have so far been investigated, among which the most active are vanadocene derivatives and peroxovanadates [11]. All these facts triggered off a lightning increase in investigations into vanadium compounds [12–14].

It is well known, that substances, which possess anti-oxidant properties, inhibit chemical carcinogenesis [15]. Thus, the combination of such ligands, for example L-cysteine, with vanadium might lead to a new generation of anticarcinogenic drugs. A literature survey revealed that only two vanadium-L-cysteine or L-cysteine methyl ester compounds were isolated and structurally characterized, namely: $[V^{IV}O(L-Cysme)_2]$ (L-HCysme = L-Cysteine methyl ester) [16], and $Na[V^{III}(L-Cys)_2] \cdot 2H_2O$ [17]. In $[V^{IV}O(L-Cysme)_2]$ the vanadium(IV) atom is ligated to two chelating Cysme⁻ ligands at the N_{amine} and S_{thiolato} atoms in a square pyramidal environment. The aqueous equilibria of the system $V^{IV}O^{2+} + L-H_2Cys$ were studied by a combination of pH-potentiometric and spectroscopic methods [18], and were corroborated by Dessi et al. [19]. It is also known that V^{IV} can be reduced to V^{III} by L-cysteine methyl ester in the presence of, for example, $edta^{4-}$ to yield $[V^{III}(edta)(H_2O)]^-$ [20].

We recently reported the significant antitumor effects of **1** on 3,4-benzopyrene induced soft tissue tumors [21,22]. Owing to the significant oxygen/water sensitivity of the vanadium(III)-L-cysteine compound, its structure remains as yet unknown. In this paper, we present the solid state characterization of compound **1** by means of microanalysis, CD and IR spectroscopies and magnetic susceptibility measurements. In addition, UV-visible, CD and EPR solution studies of **1** are described. New physiological effects of **1**, in relation to cancer treatment, are also reported. More specifically, the antimetastatic effects of **1** on tumor bearing Wistar rats were studied. According to the results discussed below, compound **1** represents the first example of a vanadium-containing species exhibiting antimetastatic effects in vivo. Moreover, biochemical properties of **1** concerning its total antioxidant capacity, lag time values as well inhibition of neutral endopeptidase (NEP) activity are presented. Neutral endopeptidase is a cell-surface enzyme that cleaves and inactivates neuro-peptides like enkephalins, implicated in the growth of some types of cancer. Compounds that inhibit both aminopeptidase and NEP were reported to prolong the effects of enkephalins, resulting in analgesia [23].

2. Experimental

2.1. Instrumentation/analytical procedures

C, H, N, S, V, and Cl analyses were conducted at Instituto Superior Técnico – Technical University of Lisbon. Vanadium was determined gravimetrically as vanadium pentoxide, and by atomic absorption. Infra-red spectra of compound **1** dispersed in KBr (Mid-IR, 4000–400 cm^{-1}) or polyethylene (Far-IR, 400–30 cm^{-1}) pellets were recorded on a Perkin–Elmer Spectrum GX FT-IR spectrometer. Magnetic moments were measured at room temperature by the Evans method, with a Johnson Matthey Alfa Products magnetic susceptibility balance. Electronic absorption spectra were measured in septum-sealed quartz cuvettes at ~ 0 °C on Jasco V-570 UV/vis/NIR, and at 25 °C on a Perkin–Elmer lambda 9 spectrophotometer. EPR spectra were recorded with frozen (77 K) solutions on a Bruker ESR-ER200D (connected to a Bruker B-MN C5) spectrometer. The CD spectra were run on a Jasco 720 spectropolarimeter with UV-vis (200–700 nm) and red-sensitive (400–1000 nm) photomultipliers. Unless otherwise stated, for isotropic absorption spectra in the 200–400 nm range or 400–1000 nm range, we use the abbreviations UV or visible spectra, respectively. For solution CD spectra a representation of $\Delta\epsilon_m$ values versus λ [$\Delta\epsilon_m$ = differential absorption/(bC_V) where b = optical path and C_V = total vanadium concentration]. For running solid state CD spectra, samples of compounds were prepared as described previously [24] in KBr disks, and placed between two microscope slides. Such paired microscope slides were placed in the sample compartment, which was kept under nitrogen. Each final spectrum is the average of four spectra recorded as previously described [24]. The position of the baseline is not exactly known and the spectra obtained are a representation of ellipticity (m deg) versus λ .

2.2. Solution spectroscopic studies

UV-visible, EPR, and CD spectra of the aqueous and methanolic solutions of compound **1** were recorded at $t = 0$ h, $t = 5$ min, $t = 10$ min, $t = 20$ min, $t = 30$ min, $t = 1$ h, $t = 1.5$ h, $t = 2$ h and every 5 h until $t = 31$ h. The solutions were prepared with non-deoxygenated solvents and they were exposed to air immediately after their preparation ($t = 0$). Solutions of compound **1** (7 mM) and sodium dithionite (20 mM) were prepared at room temperature by dissolving the solid materials in distilled water. The pH of the aqueous solution of compound **1** was ~ 3 . Addition of the sodium dithionite solution (5 ml) to the aqueous solution of compound **1** (5 ml) resulted in green solutions with pH 3.3 that were also studied as described above.

2.3. Biochemical properties

2.3.1. Measurement of total antioxidant capacity, *in vitro*

The total antioxidant capacity (TAC) of compounds $V^{IV}OSO_4 \cdot 5H_2O$, L-cysteine and **1**, was determined by using a spectrophotometric assay based on their ability to decrease ABTS [(2,2'-azino-bis-(3-ethyl-benzothiazoline-6-sulphonic acid)] oxidation to its corresponding radical cation ($ABTS^{+}$), induced by ferryl-myoglobin radicals, which were produced upon interaction of H_2O_2 with met-myoglobin as previously described [25]. The oxidation of ABTS was monitored by following the absorbance at 600 nm. The assay is standardized by the vitamin E analogue Trolox (6-hydroxy-2,5,7,8-tetramethylchroman-2-carboxylic acid) and the results are expressed as the Trolox equivalent antioxidant capacity (TEAC), which is defined as the μM concentration of a Trolox solution having the antioxidant capacity equivalent to a 1 μM solution of the substance under investigation. Lag time (in seconds), was also calculated by means of a spectrometer SHIMADZU UV-1601. Lag time was calculated from the first phase of TAC recordings and represents the time interval during which the formation of $ABTS^{+}$ radical carbocation is prevented [26]. Compound **1**, $V^{IV}OSO_4 \cdot 5H_2O$, and L-cysteine were examined for their total antioxidant capacity and lag time. According to the above assay the antioxidant capacity of solutions of $V^{IV}OSO_4 \cdot 5H_2O$, **1**, and L-cysteine in distilled water, at isomolar vanadium and L-cysteine concentrations, were measured at 10 and 300 min after solution preparation.

2.3.2. Measurement of the inhibition of neutral endopeptidase (NEP-Endophalinase) activity, *ex vivo*

The inhibition of NEP activity was measured in plasma obtained from 10 young healthy donors. The vein blood was collected in heparinized glass tubes and the plasma was separated by centrifugation (2100g for 15 min at 4 °C), just prior to the assay, as follows [27,28]: 150 μl of plasma of each sample diluted 1/10 in 0.05 M HEPES pH 7.4 buffer (HEPES = *N*-2-hydroxyethylpiperazine-*N'*-2-ethanesulfonic acid) were pre-incubated for 5 min at 37 °C, with 50 μl of the substrate Suc-Ala-Ala-Phe-AMC {succinyl-alanyl-alanyl-phenylalanyl-[(7-amino-4-methyl)-coumarine]}, at a final concentration of 10^{-4} M, dissolved in 50 mM pH 7.4 HEPES/NaOH buffer. Blank values were obtained by incubating this mixture with thiorphan (10^{-6} M), which is a NEP inhibitor. The reaction was stopped by adding 150 μl of thiorphan at a final concentration of 10^{-6} M and by heating the samples at 95 °C for 15 min. In the second step the incubation medium was further incubated at 56 °C for 60 min in the presence of 0.75 μg aminopeptidase M, previously placed at 56 °C for 60 min. After heating at 95 °C for 60 min the AMC fluorescence was measured with a Perkin-Elmer LS-S Lu-

minescence Spectrometer (at excitation of 367 nm and emission of 440 nm). In each assay the same procedure was also applied to the substrate (Suc-Ala-Ala-Phe-AMC) incubated with 3 μg of themolysin. This sample was used as a standard to determine the intensity of fluorescence after complete substrate hydrolysis. The tested substances, compound **1** and $V^{IV}OSO_4 \cdot 5H_2O$, were diluted in 0.05 M HEPES pH 7.4 buffer and added to the assay tubes with the incubation medium at final vanadium concentrations of 10^{-6} M and 10^{-3} M respectively (in the absence of thiorphan). Then, plasma samples were treated as above to measure the AMC fluorescence. Each sample was measured in triplicate. Results were expressed as percentage (%) of thiorphan inhibition of the reaction.

2.4. Physiological effects of **1**

2.4.1. Chemical carcinogenesis

For the induction of the chemical carcinogenesis, 3,4-benzopyrene was used. 3,4-benzopyrene (882 mg) was weighed and dissolved in 84 ml of tricapriline, and then a quantity of 1 ml of this solution of carcinogen was subcutaneously injected, in each rat. One millilitre of the solution contains 10.5 mg of 3,4-benzopyrene, which has been shown to induce an 100% cancer development in each rat. 3,4-benzopyrene was chosen for this experimental work because it was proved to be an efficient chemical carcinogen and gives rise to both phases of chemical carcinogenesis (initiation and promotion), without the need for a typical promoter, such as phorbol myristate acetate or croton oil, to be used. The injection of 3,4-benzopyrene was always performed at the same part of the animal body (section of the right dorsal surface of scapula dextra). It is important that the injection process is performed as described above so that the metastatic dissemination always follows the same route through the same satellite lymphonodes and the same vessels in order to reach crucial organs such as liver, lungs and brain. Diethyl ether was used for the anesthesia of the animals just prior to the 3,4-benzopyrene injection. When the anesthetized animal received subcutaneously the 3,4-benzopyrene, a metallic clip was placed at the point of the needle incision so that no 3,4-benzopyrene linkage occurs. In previous experimental work performed in our laboratory, this specific model of carcinogenesis was established. The application of this model of chemical carcinogenesis on Wistar rats results in tumor development in a percentage of 100% of the total population number of the animals used. The tumors developed appear to have a great histopathological homogeneity and are leiomyosarcomas. All the animals of the control group, that were injected this quantity of 3,4-benzopyrene in a young age (90 days old), developed tumors within 65–100 days of age and died because of the consequences of the neoplastic disease at 255–290

days of age. All of the animals used in this model of chemical carcinogenesis reacted identically due to their common genitory origin (syngenic animals), thus bearing common parental hereditary material.

2.4.2. Antimetastatic activity of $V^{IV}OSO_4 \cdot 5H_2O$, L-cysteine and compound **1**

To test whether a substance is implicated in the carcinogenic process, it can be administered before, during and after the 3,4-benzopyrene injection. If a substance possesses anticarcinogenic properties (prevention of chemical carcinogenesis), then the number of tumors in the whole animal group is reduced and an expansion of the expected life span is observed with reference to the control group. Substances able to inhibit the progression of the neoplastic malignancies are therefore anticancer agents and their administration right after the diagnosis of the tumor (through palpation) in macroscopic level, causes a reduction both in the number and the size of the tumors as far as the whole experimental animal group is concerned. If the substances used inhibit the dissemination of metastasis, then the number of metastatic tumors in different organs is also reduced. The present study focused on the investigation of tumor growth as well as on the metastatic dissemination of them. For this research, 84 male Wistar rats, three months of age and with body weight in the range of 250–300 g, were used. The animals were supplied from the animal breeding center of the University of Ioannina. The tested animals had common genitory origin. These Wistar rats were separated into four groups of 21 animals each. Each one of these groups included animals of similar body weight. The four groups were: the control group 1 that received only the injection of 3,4-benzopyrene (10.5 mg of 3,4-benzopyrene/ml tricaprilin/animal), the $V^{IV}OSO_4 \cdot 5H_2O$ group 2, the L-cysteine group 3 and the compound **1** group 4. The groups 2–4 were also received the injection of 3,4-benzopyrene. After the macroscopic appearance of the tumor, the animals of the groups 2 and 4 received per os a quantity of 0.5 ± 0.18 mg of vanadium/kg bw/day up to the day of their death in the form of $V^{IV}OSO_4 \cdot 5H_2O$ and of **1** respectively. Group 3 received per os L-cysteine in equivalent quantities to those contained in **1**. Both $V^{IV}OSO_4 \cdot 5H_2O$ and compound **1** were dissolved in tap water and fresh solutions were prepared every day. The animals of the control group received only tap water. The administration of the solutions started as soon as the tumor was detected by palpation in each animal and continued up to the day of their death. The diagnostic palpation of the animals started 40 days after the 3,4-benzopyrene injection and was performed three times a week. The animals were weighed once a week and had their temperature taken at the same time. The animals that were about to die were placed in separate cages (one animal per cage) and were observed three times a day (every 8 h). The rest of the

animals were observed only once a day. Animals that appeared to have inflammatory disease were isolated and received anti-inflammatory treatment. The treatment was given without stopping the administration of the vanadium compound **1**. Fortunately there was no such incidence during the study, except for one animal of the control group. Soon after their death, each animal was weighed and an autopsy was performed. The brain, lungs, liver, stomach, intestine and kidneys were isolated, weighed, and stored in a formaldehyde solution (8%) for the histological examination. The histological analysis aimed at: (1) finding possible metastases and (2) the determination of animal's death cause. The developed tumors were carefully excised, weighed, and prepared for histological examination.

2.5. Materials

Reagent grade chemicals were obtained from Aldrich and were used without further purification. Methyl alcohol was dried by refluxing over magnesium methoxide, while diethyl ether was dried and distilled over sodium wire.

2.6. Synthesis

2.6.1. Preparation of the vanadium(III)-L-cysteine compound **1**

Vanadium(III) chloride (1.00 g, 6.35 mmol) was dissolved in methyl alcohol (25 ml) under argon and magnetic stirring, at ambient temperature. Solid L-cysteine (2.31 g, 19.07 mmol) was added to the solution in one portion. Upon addition of L-cysteine, the green color of the solution changed to olive green. The resulting mixture was allowed to stir for 3 h, during which L-cysteine was fully dissolved and a brown precipitate was formed (pH \sim 2). The brown solid was filtered off and washed with cold methyl alcohol (2×10 ml) and diethyl ether (2×10 ml) and dried in vacuo. Yield: 1.68 g (50%). Found: C, 20.11; H, 4.46; N, 7.20; S, 17.95; Cl, 13.70; V, 10.1. Calc. for ($C_9H_{25}Cl_2N_3O_{8.5}S_3V$): C, 20.42; H, 4.76; N, 7.94; S, 18.17; Cl, 13.40; V, 9.62.

3. Results and discussion

3.1. Solid state characterization of compound **1**

Despite our efforts, the crystallization of **1** for X-ray diffraction studies has been proven unsuccessful thus far. However, the several C, H, N, S, Cl and V analyses that were done were consistent with the formula $[V^{III}(HCys)_3] \cdot 2HCl \cdot 2.5H_2O$. The infrared spectrum of compound **1** exhibited a weak-to medium intensity broad band at ≈ 3400 cm^{-1} , which was assigned to $\nu(OH)$ arising from the lattice water molecules. The S–H

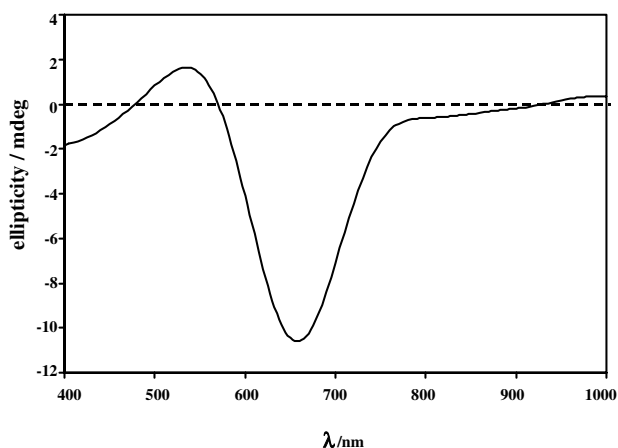


Fig. 1. CD spectrum of a solid sample of compound **1** dispersed in a KBr disk.

stretching vibration appeared as a weak shoulder at $\sim 2550\text{ cm}^{-1}$, and this indicated that the S–H proton is possibly involved in H-bonds with water oxygen atoms. The $\nu_{\text{as}}(\text{COO}^-)$ and $\nu_{\text{s}}(\text{COO}^-)$ bands appeared at 1607 and 1349 cm^{-1} , respectively. The relatively large Δ value [$\Delta = \nu_{\text{as}}(\text{COO}) - \nu_{\text{s}}(\text{COO}) = 258\text{ cm}^{-1}$] [29] is indicative of a monodentate carboxylate coordination. The Far-IR ($400\text{--}30\text{ cm}^{-1}$) spectrum of compound **1** contained no peaks in the region $340\text{--}370\text{ cm}^{-1}$, where the V–Cl absorption is usually expected [30]. This might be an indication that the V^{III} center does not contain any terminal chlorine atoms in its coordination sphere and thus the chlorine content of **1** (determined by ion-chromatography analysis) should be due to lattice HCl molecules or bridging chlorine atoms.¹ In addition, the magnetic moment of **1** is $\sim 2.60\ \mu_{\text{B}}$ at 298 K, in agreement with the spin-only value expected for d^2 systems. The CD spectrum of the solid **1** (Fig. 1) does not clearly correspond to an oxovanadium(IV) compound. The CD spectra of oxovanadium(IV) complexes typically contain two bands at ≈ 550 and 740 nm [24]; however, in the CD spectrum of **1** at least four bands are present in the range 400–1000 nm (Fig. 1). The intensity of the CD bands, particularly at 657 nm, which corresponds to a relatively high rotatory strength [31], indicated that L-HCys[−] is coordinated to vanadium as a bidentate ligand.

¹ The absence of a $\nu(\text{V}\text{--}\text{Cl})$ stretch in the Far-IR spectrum of compound **1**, does not rule out the possibility of V–Cl bonds being present. Assuming that there are V–Cl bonds in compound **1**, then several other formulations could be proposed. For example the formulation $[\text{V}^{\text{III}}(\text{HCys})_2\text{Cl}_2]^- \cdot \text{H}_3\text{Cys}^+ \cdot 2.5\text{H}_2\text{O}$ is also reasonable (H_3Cys^+ is a lattice protonated cysteine cation). Alternatively, dimeric-type structures could also be proposed, e.g. $[\text{V}^{\text{III}}(\text{HCys})_2(\mu\text{--}\text{Cl})_2\text{V}^{\text{III}}(\text{HCys})_2] \cdot (\text{H}_3\text{Cys}^+)_2\text{Cl}_2 \cdot 2.5\text{H}_2\text{O}$, with two bridging chlorine ligands. However, if H_3Cys^+ cations were present, then the $\nu(\text{C}=\text{O})_{\text{COOH}}$ stretches should be observed in the range of $1700\text{--}1750\text{ cm}^{-1}$, but in the IR spectrum of compound **1** only a weak/medium shoulder was recorded at about 1750 cm^{-1} .

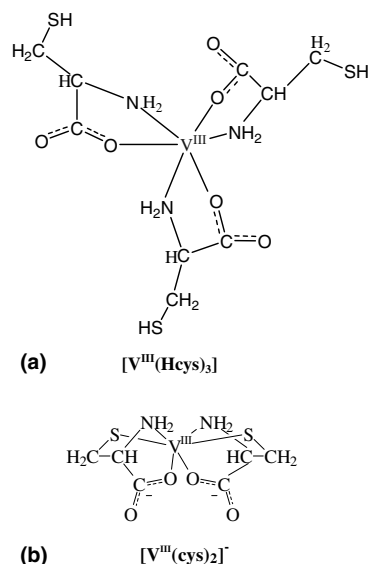


Fig. 2. The structures of $[\text{V}^{\text{III}}(\text{HCys})_3]$ (a) and of $[\text{V}^{\text{III}}(\text{Cys})_2]^-$ (b) (from [17]).

Based on all the above mentioned solid state measurements, we propose that **1** corresponds to a six-coordinate V^{III} complex (Fig. 2(a)) with the V^{III} center coordinated to three carboxylate oxygen and three amine nitrogen atoms provided by three HCys[−] chelating ligands. The structurally characterized $[\text{V}^{\text{III}}(\text{Cys})_2]^-$ species [17] shows that the vanadium(III) atom is ligated to two bis-chelate tridentate cys^{2-} ligands at the N_{amine} , $\text{S}_{\text{thiolato}}$, $\text{O}_{\text{carboxylato}}$ atoms (Fig. 2(b)). However, the preparation of $[\text{V}^{\text{III}}(\text{Cys})_2]^-$ was done in aqueous solution at $\text{pH} \sim 7$, while the preparation of $[\text{V}^{\text{III}}(\text{HCys})_3]$ was performed in methyl alcohol solution and at $\text{pH} \sim 2$.

3.2. Solution spectroscopic studies of compound **1**

The CD spectrum of **1** in water immediately after its preparation ($t = 0$) was very weak and contained four bands in the range 400–1000 nm at ~ 455 , ~ 590 , ~ 655 and ~ 930 nm, with $\Delta\epsilon_m$ values of $+0.0007$, -0.006 , -0.006 and $-0.002\text{ M}^{-1}\text{ cm}^{-1}$, respectively. The bands at ~ 590 and ~ 655 nm appeared as broad bands with an apparent maximum at ~ 630 nm. The corresponding visible spectrum of **1** in water showed a distinct band at 433 ($\epsilon = 145\text{ M}^{-1}\text{ cm}^{-1}$), and two shoulders at 335 nm ($\epsilon = 68\text{ M}^{-1}\text{ cm}^{-1}$) and 666 nm ($\epsilon = 20\text{ M}^{-1}\text{ cm}^{-1}$) (Fig. 3), while the visible spectrum of $[\text{V}^{\text{III}}(\text{Cys})_2]^-$ in water showed two bands at 580 nm (weak) and 420 nm (very intense), assigned to d–d and LMCT bands, respectively [17]. However the latter spectrum was recorded in a solution containing a 50-fold excess of L-cysteine. The CD spectrum of **1** in methyl alcohol immediately after its preparation was stronger in intensity (more than 10 times) than its spectrum in water, and

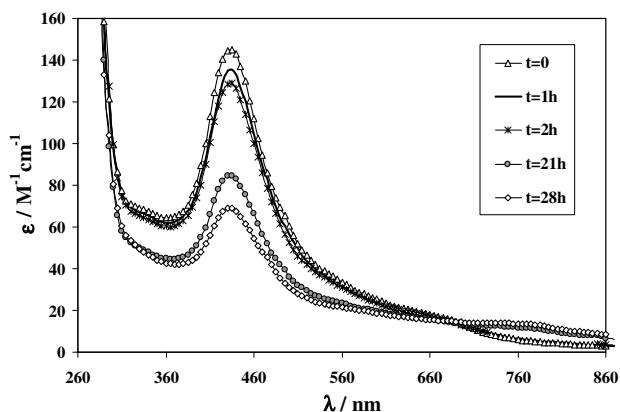


Fig. 3. Visible spectra of compound **1** in water at $t = 0, 1, 2, 21,$ and 28 h after its preparation. The ϵ (epsilon) values correspond to absorbance/(total vanadium concentration).

showed bands at $\sim 400, \sim 440, 505$ and 645 nm, with $\Delta\epsilon_m$ values of $+0.030, -0.027, -0.022$ and -0.267 $\text{M}^{-1} \text{cm}^{-1}$, respectively. Its corresponding visible spectrum contained bands at 400 nm ($\epsilon = 190$ $\text{M}^{-1} \text{cm}^{-1}$) and ~ 570 (sh) nm ($\epsilon = 40$ $\text{M}^{-1} \text{cm}^{-1}$).

In water, the EPR, CD and visible spectra of **1** (Fig. 3 and Table 1) indicate a progressive and consistent change from V^{III} to V^{IV} species. The EPR at $t = 0$ h showed a relatively strong signal ($g_z = 1.938, A_z = 181.4 \times 10^{-4} \text{ cm}^{-1}$), and its intensity increased with time. At $t = 31$ h the EPR parameters were identical, within experimental error, to those observed at $t \sim 0$ h. All these EPR results are in agreement with the equi-

Table 1

Values of Δ , Racah (B) and nephelauxetic (β) parameters obtained [34] from visible and CD data of compound **1** in water and methyl alcohol, immediately after its dissolution ($t \sim 0$ h)

$t \sim 0$ (h)	B (cm^{-1})	Δ (cm^{-1})	β^c
Vis in water ^{a,b}	621	16,270	0.722
Vis in methanol	576	18,893	0.670
CD in water	521	16,360	0.606
CD in methanol ^b	570	16,714	0.662

^a In the range $320\text{--}900$ nm there are a distinct λ_{max} (lambda max) at ~ 433 nm, and two shoulders at ~ 335 and ~ 666 nm (see Fig. 3). The λ values at 433 and 666 nm were used for the calculations of Δ and B .

^b It is difficult to get a correct λ_{max} of the band near 660 nm. Other λ_{max} would lead to different B values.

^c The free-ion value of the Racah parameter B for $\text{V}(\text{III})$ is 860 cm^{-1} [34].

librium models reported in the literature [18] for the $\text{V}^{\text{IV}}\text{O}^{2+}\text{-Cys}$ system at the same pH (~ 3) and with a ligand-to-metal ratio of 3. However, under these EPR spectra two $\text{V}^{\text{IV}}\text{O}^{2+}$ -species are hidden [18]: the aquation, $[\text{V}^{\text{IV}}\text{O}(\text{H}_2\text{O})_5]^{2+}$, and a $\text{V}^{\text{IV}}\text{O}^{2+}\text{-Cys}$ complex (Fig. 4, species **A**), as evidenced by the parallel line widths at $M_z = 7/2$ and the CD spectra (see below). Species **A** contains a protonated L-cysteine ligand coordinated to the V^{IV} center through a monodentate carboxylate group and four water ligands, in addition to the O_{oxo} (Fig. 4) [18].

Thus, the oxidation of **1** in water results not only in the formation of the aqua complex $[\text{V}^{\text{IV}}\text{O}(\text{H}_2\text{O})_5]^{2+}$, but also in the formation of species **A** (Fig. 4). The existence of species **A** in the aqueous solution of **1** was also con-

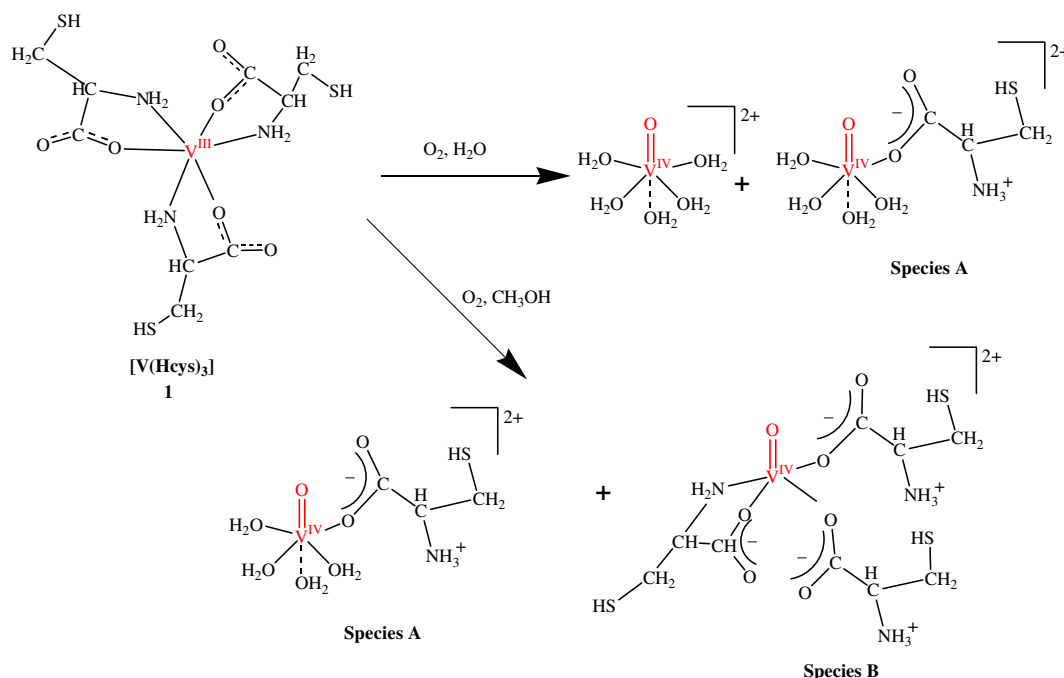


Fig. 4. The oxidation products of compound **1** in H_2O and CH_3OH . The proposed structures were based on cw EPR and CD measurements and [18].

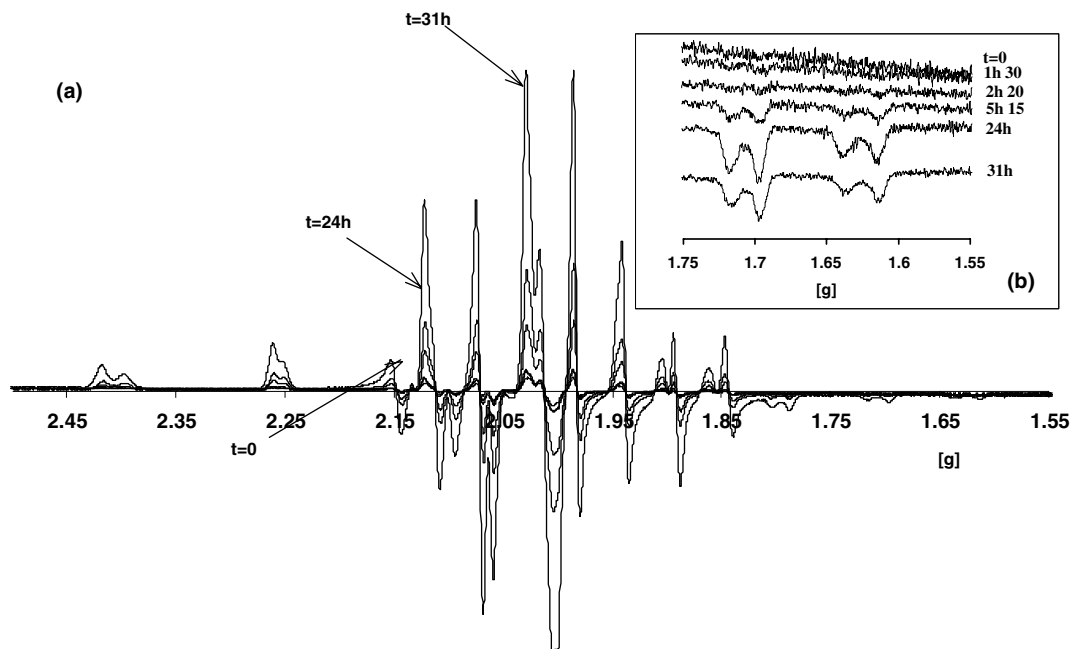


Fig. 5. (a) cw EPR spectra of solutions of compound **1** at 77 K in CH_3OH at $t = 0$ h, 1 h and 30 min, 2 h and 20 min, 5 h and 15 min, 24 and 31 h after the preparation of the solution of compound **1**. The intensity of the EPR signals increases with time. (b) The formation of the two different species is emphasized by amplification of the signals in the high field region.

firmed by its CD spectrum at $t = 31$ h. This spectrum was extremely weak, but it was in agreement with the CD spectrum of species **A** [18]. The visible spectrum of the aqueous solution of **1**, at $t = 28$ h (Fig. 3), and in particular the pattern of the absorption in the range 400–600 nm, revealed that besides the oxovanadium(IV) complexes mentioned above, some other species are also present. Presumably there was a significant amount of V(III)-containing species from which the absorptions originated in this range, particularly around 430 nm.

The oxidation of **1** in methyl alcohol was much slower. The solution CD spectrum of **1** in methyl alcohol at $t \sim 0$ h was similar to its CD spectrum in the solid state and the EPR signals in methyl alcohol were weak, increasing significantly with time. Fig. 5 shows the variation of the EPR spectra with time, and the high field region where the presence of two oxovanadium(IV) species, with $g_z = 1.939$, $A_z = 179.0 \times 10^{-4} \text{ cm}^{-1}$ and $g_z = 1.947$, $A_z = 169 \times 10^{-4} \text{ cm}^{-1}$, is obvious. Application of the additivity relationship [32,33] to the equatorial binding modes ($4\text{H}_2\text{O}$) and ($3\text{H}_2\text{O}$, 1RCOO^-) yields calculated A_z values of 182.6 and $179 \times 10^{-4} \text{ cm}^{-1}$, respectively. The calculated A_z of $179 \times 10^{-4} \text{ cm}^{-1}$ coincides with the experimental value of $179.0 \times 10^{-4} \text{ cm}^{-1}$ and thus, it is reasonable to assume that this signal corresponds to species **A** (Fig. 4). Application of the additivity relationship to an equatorial binding mode (3RCOO^- , 1RNH_2) yields a calculated A_z value of $168.2 \times 10^{-4} \text{ cm}^{-1}$, i.e., very close to the experimental value of $169 \times 10^{-4} \text{ cm}^{-1}$. Thus, the second species de-

tected in the EPR spectrum in methyl alcohol, having the parameters $g_z = 1.947$, $A_z = 169 \times 10^{-4} \text{ cm}^{-1}$, should be the species **B** (Fig. 4).

The visible spectra of methanolic solutions of **1** initially showed a shift of the band at ~ 400 to ~ 420 nm. After almost 1 h the intensity of the 420 nm band progressively decreased. The absorption of a $\text{V}^{\text{IV}}\text{O}^{2+}$ -species at 400–420 nm would be almost zero. After ~ 31 h the band at 420 nm was still not zero and this was consistent with the existence of some V^{III} species in solution. From the initial visible spectra B , Δ and β parameters could be calculated (see Table 1) [34]. The absorption in the range 720–900 nm, mainly due to $\text{V}^{\text{IV}}\text{O}^{2+}$ -complexes, was initially very weak and progressively increased with time.

Some additional experiments were also done, with the presence of a strong reducing agent, such as sodium dithionite, in order to study its effectiveness in preventing the oxidation of **1**. However, trying to dissolve complex **1** in water, containing 20 mM of Na-dithionite, a suspension was formed, i.e. it appeared that **1** was not significantly soluble in water in the presence of the reducing agent. Complex **1** was therefore first dissolved in water (7.2 mM) forming a light-brown solution and its visible spectrum exhibited a band at ~ 430 nm and a shoulder at ~ 660 nm, as shown in Fig. 3 ($t \sim 0$ h). Sodium dithionite was then added in a 3:1 (Na-dithionite:vanadium) molar ratio and the color of the solution changed to green. The visible spectrum recorded immediately after the addition of the reducing agent

exhibited a shoulder (instead of a band) at ~ 430 nm ($\epsilon = 50 \text{ M}^{-1} \text{ cm}^{-1}$), as well as a distinct band at ~ 600 nm ($\epsilon = 18 \text{ M}^{-1} \text{ cm}^{-1}$). The visible spectra did not change significantly within the first 3 h after addition of Na-dithionite. The intensity of the band at ~ 600 nm was decreasing slightly with time, while a band with $\lambda_{\text{max}} = 760$ nm progressively developed. Twenty six hours after the Na-dithionite addition the band at ~ 600 nm was still present, now with $\epsilon = 14 \text{ M}^{-1} \text{ cm}^{-1}$, thus indicating the presence of a substantial amount of V(III) species. An additional band with $\lambda_{\text{max}} = 760$ nm and $\epsilon = 15 \text{ M}^{-1} \text{ cm}^{-1}$ also appeared, which indicated the formation of an important amount of $\text{V}^{\text{IV}}\text{O}^{2+}$ species. The CD spectra of these solutions were very weak at the beginning, and became progressively stronger. After $t = 20$ h their intensity was higher than that of the corresponding spectra in the experiment without Na-dithionite addition. Moreover, the EPR spectra showed a significant signal since the beginning, and their intensity increased with time. However the g_z , A_z parameters did not change ($g_z = 1.940$, $A_z = 178.5 \times 10^{-4} \text{ cm}^{-1}$), indicating that the $\text{V}^{\text{IV}}\text{O}^{2+}$ -complexes present consisted of a mixture of $[\text{V}^{\text{IV}}\text{O}(\text{H}_2\text{O})_5]^{2+}$ and species **A** (Fig. 4).

The spectroscopic results in solution indicate that the thiolate sulfur is not coordinated to the V^{III} center in compound **1**. In addition, it seems that **1** only dissolves in water upon partial oxidation. Such an oxidation of **1** also occurred in methyl alcohol, but at a lower degree and rate. Na-dithionite delayed the oxidation process. It is also noteworthy that in both methyl alcohol and water, some complex species containing V^{III} persisted for many hours. Taking into account the existence of a band at 410–430 nm in the visible spectra of solutions of **1** (see Fig. 3), we conclude that this species is probably a dinuclear V(III)–O–V(III) complex [35–37].

3.3. Biochemical properties and physiological effects of compound **1**

An ideal anticancer drug should possess the following characteristics: potent cytotoxicity on malignant cells, low toxicity and reduced side effects, antimetastatic action and if possible analgesic effects. Substances with antioxidant properties may help to prevent drug-induced toxicity by free radical production. Substances that may inhibit platelet aggregation may also prevent metastasis. To achieve analgesia one can either increase the production of endorphins or inhibit the catabolism through inhibition of their specific catabolizing enzyme, neutral endopeptidase (NEP). Complex **1** was tested for such biochemical and physiological effects. The total antioxidant capacity and lag time of the tested substances are shown in Table 2. According to these results, $\text{V}^{\text{IV}}\text{OSO}_4 \cdot 5\text{H}_2\text{O}$ had no total antioxidant capacity or lag time. In contrast, L-cysteine in water possesses TAC and lag time properties, which progressively disappeared

Table 2

TAC and lag time values of $\text{V}^{\text{IV}}\text{OSO}_4 \cdot 5\text{H}_2\text{O}$, L-cysteine and compound **1**

Substances	Time from solution preparation (min)	TAC (μM)	Lag time (s)
$\text{V}^{\text{IV}}\text{OSO}_4 \cdot 5\text{H}_2\text{O}$	10	0.000	00.0
L-cysteine	10	0.430	36.0
L-cysteine	300	0.000	00.0
1	10	0.760	38.4
1	300	0.680	35.2

Table 3

Percentage of inhibition of NEP-activity caused by Thiorphan, $\text{V}^{\text{IV}}\text{OSO}_4 \cdot 5\text{H}_2\text{O}$ and **1**

Substances	Concentration	% Inhibition
Thiorphan	10^{-6} M	101.1 ± 9.5
$\text{V}^{\text{IV}}\text{OSO}_4 \cdot 5\text{H}_2\text{O}$	10^{-6} M	18.7 ± 9.2
$\text{V}^{\text{IV}}\text{OSO}_4 \cdot 5\text{H}_2\text{O}$	10^{-3} M	38.6 ± 11.2
1	10^{-6} M	74.3 ± 15.2
1	10^{-3} M	119.5 ± 29.6

after 10 min, due to the rapid oxidation of L-cysteine. Compound **1** in water possesses high TAC and lag time values (0.760 mM, 38.4 s, respectively), which were maintained for long time (at least for 5 h). The latter could be explained by the chemical properties of complex **1**, which protects L-cysteine from oxidation for a long period of time, whereas L-cysteine alone is rapidly oxidized.

Percentages of inhibition of NEP-activity in human plasma caused by thiorphan, $\text{V}^{\text{IV}}\text{OSO}_4 \cdot 5\text{H}_2\text{O}$ and compound **1** are given in Table 3. According to these results, compound **1** manifests a remarkable *ex vivo* inhibition of NEP activity in comparison to isomolar concentrations of thiorphan, whereas $\text{V}^{\text{IV}}\text{OSO}_4 \cdot 5\text{H}_2\text{O}$ exhibits a significantly lower inhibition at the same vanadium concentrations ($P < 0.001$). Solutions of compound **1** at concentrations 10^{-3} M, result in an inhibition of NEP activity as high as thiorphan at a concentration of 10^{-6} M, whereas $\text{V}^{\text{IV}}\text{OSO}_4 \cdot 5\text{H}_2\text{O}$ at the same concentration, exhibits an inhibitory activity less than 50% of that of thiorphan (10^{-6} M).

The antimetastatic effects of **1**, $\text{V}^{\text{IV}}\text{OSO}_4 \cdot 5\text{H}_2\text{O}$ and L-cysteine on tumor bearing Wistar rats were also examined. All animals except four of them (19%) in the group treated with compound **1** were found to bear tumors at the site of injection, which were histologically defined as leiomyosarcomas. Metastases were histologically identified only in lungs of the animals of all groups. The number and the percentage of animals with lung metastasis in each group are shown in Table 4. These results revealed that animals treated with **1** showed a significantly higher prevention of lung metastases (incidence: 9.5%) when compared to groups treated with $\text{V}^{\text{IV}}\text{OSO}_4 \cdot 5\text{H}_2\text{O}$ and L-cysteine, as well as

Table 4

Number and percentage of animals exhibiting lung metastasis in groups treated with $V^{IV}OSO_4 \cdot 5H_2O$, L-cysteine and compound **1** as well as in the control group

Groups	Number of animals (<i>N</i> = 21)	Percentage (%)	Significance (<i>P</i>)
Control	11/21	52.4	–
$V^{IV}OSO_4 \cdot 5H_2O$	11/21	52.4	NS
L-cysteine	10/21	47.1	NS
1	2/21	9.5	<0.001 ^a

^a Compared to the control and the other groups.

the control group, in which metastases were found in 47–52% of the animals (see Table 4).

4. Conclusion

In summary, the solid state studies of compound **1** by means of microanalysis, circular dichroism and infrared spectroscopy as well as room temperature magnetic susceptibility measurements were consistent with a V^{III} complex, containing three bidentate $Hcys^-$ ligands each ligated to vanadium(III) through an amine nitrogen and a carboxylate oxygen atoms. The solution behavior of **1** showed that the complex seems to be partially oxidized after its dissolution in water and the amount of $V^{IV}O^{2+}$ species formed progressively increased with time. However, a significant amount of a V^{III} species, which probably corresponds to a dinuclear $V(III)-O-V(III)$ species, was present in solution even after 31 h of the dissolution of **1** in water. In addition, taking into account that $V^{IV}OSO_4 \cdot 5H_2O$ shows no TAC and lag time, low inhibition of NEP activity and low antimetastatic effects, we propose that the antitumor activity of compound **1** is probably due to the $V(III)$ containing species present in solution, rather than $V^{IV}O^{2+}$ ones or L-cysteine molecules. However, we cannot exclude the contribution of L-cysteine molecules in the biochemical properties of compound **1** as efficient inhibitor of NEP activity, high total antioxidant capacity and possibly inhibition of platelet aggregation, contributing to its antimetastatic effect [38].

The biochemical and physiological studies reported in this paper have shown significant total antioxidant capacity, lag time values and inhibition of NEP activity for compound **1**. In marked contrast to $V^{IV}OSO_4 \cdot 5H_2O$ and L-cysteine, compound **1** significantly prevents lung metastasis, thus being the first example of a vanadium-containing species exhibiting antimetastatic effects in vivo. Compound **1** might combine the anticancer properties of a metal ion (i.e. vanadium) with the anticancer properties of an antioxidant (i.e. L-cysteine), thus overcoming the need to use antioxidants in megadoses. Therefore, the combination of some antioxidants, such

as sulfhydryl containing organic ligands, with trace elements, such as vanadium, might result in a new generation of anticancer drugs. One of our strategies in order to understand the mechanism of the biological activity of compound **1** is to synthesize new more stable vanadium(III)-sulfhydryl compounds that will allow us to do more quantified biological studies.

5. Abbreviations

H_2Cys	L-cysteine
L-HCysme	L-cysteine methyl ester
H_4edta	ethylenediaminetetraacetic acid
$\Delta\epsilon_m$	differential absorption
ABTS	2,2'-azinobis-(3-ethyl-benzothiazoline-6-sulphonic acid)
Trolox	6-hydroxy-2,5,7,8-tetramethylchroman-2-carboxylic acid
TEAC	Trolox equivalent antioxidant capacity
HEPES	<i>N</i> -2-hydroxyethylpiperazine- <i>N'</i> -2-ethane sulfonic acid
AMC	(7-amino-4-methyl)-coumarine
CD	circular dichroism
EPR	electron paramagnetic resonance
TAC	total antioxidant capacity
NEP	neutral endopeptidase activity

Acknowledgements

We gratefully acknowledge support of this research by the D21 COST Program. J.C.P. and I.C. are grateful to the Fundo Europeu para o Desenvolvimento Regional, Fundação para a Ciência e Tecnologia and the POCTI Programme (project POCTI/35368/QUI/2000).

References

- [1] P. Frank, R.M.K. Carlson, E.J. Carlson, K. Hodgson, *Coord. Chem. Rev.* 237 (2003) 31–39.
- [2] R.E. Berry, E.M. Armstrong, R.L. Beddoes, D. Collison, S.N. Ertok, M. Helliwell, C.D. Garner, *Angew. Chem. Int. Ed.* 38 (1999) 795–797.
- [3] D. Rehder, *Inorg. Chem. Commun.* 6 (2003) 604–617.
- [4] R.R. Eady, *Coord. Chem. Rev.* 237 (2003) 23.
- [5] A. Messerschmidt, R. Wever, *Proc. Natl. Acad. Sci. USA* 93 (1996) 392.
- [6] A.N. Antipov, D.Y. Sorokin, N.P. L'Lov, J.G. Kuenen, *Biochem. J.* 369 (2003) 185–189.
- [7] P.J. Stankiewicz, A.S. Tracey, D.S. Crans, in: Vanadium and its role in life, in: H. Sigel, A. Sigel (Eds.), *Metal Ions in Biological Systems*, vol. 31, Marcel Dekker, New York, 1995 (Chapter 9).
- [8] G.L. Mendz, *Arch. Biochem. Biophys.* 291 (1991) 201–211.
- [9] S.A. Dikanov, B.D. Liboiron, C. Orvig, *J. Am. Chem. Soc.* 124 (2002) 2969–2978.
- [10] A. Bishayee, R.M. Chatterjee, *Anticancer Res.* 15 (1995) 455–461.

- [11] C. Djorgevitz, in: H. Sigel, A. Sigel (Eds.), *Metal Ions in Biological Systems*, vol. 31, Marcel Dekker, New York, 1995, pp. 596–616.
- [12] M. Kaliva, E. Kyriakakis, A. Salifoglou, *Inorg. Chem.* 41 (2002) 7015.
- [13] D.C. Crans, L. Yang, T. Jakusch, T. Kiss, *Inorg. Chem.* 39 (2000) 4409–4416.
- [14] E. Garribba, G. Micera, A. Panzanelli, D. Sanna, *Inorg. Chem.* 42 (2003) 3981–3987.
- [15] A. Evangelou, G. Kalpouzou, S. Karkabounas, R. Lasko, A. Nonni, D. Stefanou, G. Kallistratos, *Cancer Lett.* 115 (1997) 105–111.
- [16] H. Sakurai, Z. Taira, N. Sakai, *Inorg. Chim. Acta* 151 (1988) 85–86.
- [17] H. Maeda, K. Kanamori, H. Michibata, T. Konno, K. Okamoto, J. Hidaka, *Bull. Chem. Soc. Jpn.* 66 (1993) 790–796.
- [18] J.C. Pessoa, L.F. Vilas Boas, R.D. Gillard, *Polyhedron* 9 (1990) 2101–2125.
- [19] A. Dessi, M. Micera, D. Sanna, *J. Inorg. Biochem.* 52 (1993) 275–286.
- [20] K. Kanamori, Y. Kinebuchi, H. Michibata, *Chem. Lett.* 14 (1997) 423–424.
- [21] R. Liasko, T.A. Kabanos, S. Karkabounas, M. Malamas, A.T. Tasiopoulos, D. Stefanou, P. Collery, A. Evangelou, *Anticancer Res.* 18 (1998) 3609–3614.
- [22] A. Evangelou, S. Karkabounas, G. Kalpouzou, M. Malamas, R. Liasko, D. Stefanou, A.T. Vlahos, T.A. Kabanos, *Cancer Lett.* 119 (1997) 221–225.
- [23] E.G. Erdos, R.A. Skidgel, *FASEB J.* 3 (1989) 145–151.
- [24] I. Cavaco, J.C. Pessoa, M.T. Duarte, R.T. Henriques, P.M. Matias, R.D. Gillard, *J. Chem. Soc. Dalton Trans.* (1996) 1989–1996.
- [25] C. Rice-Evans, N.J. Miller, *Meth. Enzymol.* 234 (1994) 279–293.
- [26] K. Schlesier, M. Harwat, V. Bohm, R. Bitsch, *Free Radic. Res.* 36 (2002) 177–187.
- [27] M.G. Spillatini, F. Sicuteri, S. Salmon, B. Malfroy, *Chem. Pharmacol.* 39 (1990) 1353–1356.
- [28] M.G. Spillatini, P. Geppetti, M. Fanciullacci, S. Michelacci, J.M. Lecomte, F. Sicuteri, *Eur. J. Pharmacol.* 125 (1986) 147–150.
- [29] K. Nakamoto, *Infrared and Raman Spectra of Inorganic and Coordination Compounds*, fourth ed., Wiley, New York, 1986, pp. 227–244.
- [30] A. Keramidas, A. Papaioannou, A. Vlahos, T. Kabanos, G. Bonas, A. Makriyannis, C. Raptopoulou, A. Terzis, *Inorg. Chem.* 35 (1996) 357–367.
- [31] R.D. Gillard, in: H. Hill (Ed.), *Physical Methods in Advanced Inorganic Chemistry*, Interscience, 1969, pp. 167–213.
- [32] A.J. Tasiopoulos, A.N. Troganis, A. Evangelou, C.P. Raptopoulou, A. Terzis, Y. Deligiannakis, T.A. Kabanos, *Chem. Eur. J.* 5 (1999) 910–921, and references therein.
- [33] N.D. Chasteen, in: L.J. Berliner, J. Reuben (Eds.), *Biological Magnetic Resonance*, vol. 3, Plenum, New York, 1981, pp. 53–119.
- [34] S.F.A. Kettle, *Physical Inorganic Chemistry, A Coordination Chemistry Approach*, Spektrum, 1996, pp. 159–160.
- [35] G. Micera, D. Sanna, in: J.O. Nriagu (Ed.), *Spectroscopic Methods for the Characterization of Vanadium Complexes, Vanadium in the environment Part 1*, vol. 30, John Wiley and Sons, New York, 1998, pp. 131–166.
- [36] K. Kanamori, M. Teraoka, H. Maeda, K. Okamoto, *Chem. Lett.* 10 (1993) 1731–1734.
- [37] R.S. Czernuszewicz, Q. Yan, M.R. Bond, C.J. Carrano, *Inorg. Chem.* 33 (1994) 6116–6119.
- [38] A. Evangelou, *Crit. Rev. Oncol. Hematol.* 42 (2002) 249–265.